applied sciences

MDPI

Review

Metal Matrix Composite Fabricated with 5000 Series Marine Grades of Aluminium Using FSP Technique: State of the Art Review

Oritonda Muribwathoho *, Velaphi Msomi * and Sipokazi Mabuwa

Mechanical Engineering Department, Cape Peninsula University of Technology, Cape Town 7535, Western Cape, South Africa
* Correspondence: oritondamuribwathoho@gmail.com (O.M.); msomiv@gmail.com (V.M.)

Abstract: Aluminium metal matrix composites have been shown to make significant contributions to the area of new materials and have become widely accepted in high-tech structural and functional applications such as those in the aircraft, automobile, marine, mineral, defence, transportation, thermal management, automotive, and sports and recreation fields. Metal matrix composites are manufactured using a variety of manufacturing processes. Stirring casting, powder metallurgy, squeezing casting, in situ processes, deposition techniques, and electroplating are part of the manufacturing process used in the manufacture of aluminium-metal matrix composites. Metal matrix composites that use friction stir processing have a distinct advantage over metal matrix composites that use other manufacturing techniques. FSP's benefits include a finer grain, processing zone homogeneity, densification, and the homogenization of aluminium alloy and composite precipitates. Most metal matrix composite investigations achieve aluminium-metal matrix composite precipitate grain refinement, treated zone homogeneity, densification, and homogenization. This part of the work examines the impact of reinforcing particles, process parameters, multiple passes, and active cooling on mechanical properties during the fabrication of 5000-series aluminium-metal matrix composites using friction stir processing. This paper reports on the available literature on aluminium metal matrix composites fabricated with 5xxx series marine grade aluminium alloy using FSP.

Keywords: aluminium 5xxx series; marine grades; friction stir welding; friction stir processing; composite; metal matrix composite

check for updates

Citation: Muribwathoho, O.; Msomi, V.; Mabuwa, S. Metal Matrix Composite Fabricated with 5000 Series Marine Grades of Aluminium Using FSP Technique: State of the Art Review. *Appl. Sci.* **2022**, *12*, 12832. https://doi.org/10.3390/app122412832

Academic Editor: Jacek Tomków

Received: 24 October 2022
Accepted: 10 December 2022
Published: 14 December 2022

Publisher's Note: MDPI stays neutral with regard to jurisdictional claims in published maps and institutional affiliations.

Copyright: © 2022 by the authors. Licensee MDPI, Basel, Switzerland. This article is an open access article distributed under the terms and conditions of the Creative Commons Attribution (CC BY) license (https://creativecommons.org/licenses/by/4.0/).

1. Introduction

Aluminium alloys have exceptional flexibility and applicability, along with multiple benefits (corrosion resistance, strength, and workability), making them suitable for a variety of goods and markets [1]. Naval architects and ocean engineers have recognized aluminium and its alloys as very favourable materials for marine and offshore structures [2]. The improved, lighter-weight mechanical properties and corrosion resistance of aluminium alloys have made many of these applications possible. Naval architects can use aluminium to build boats that have a longer life, a high recycling value, minimal maintenance costs, higher payloads, and high-speed capability [3]. In shipbuilding, several marine AAs are used to fabricate various sections, such as hulls, superstructures, decks, and bulkheads. Aluminium and its alloys provide significant benefits in terms of hull maintenance and structural weight reduction [4].

The 5xxx series of aluminium magnesium alloys, one of the most significant series of aluminium alloys, have found wide use in the automotive and transportation sectors, aerospace aluminium panels, and marine applications due to their advantageous properties, particularly corrosion resistance and weldability [5–7]. Aluminium alloys from the 5xxx series have appropriate corrosion-resistance properties and strength, making them popular materials for decks, ship-hull constructions, corrosive environments, superstructures, and

other components [8,9] and are used in many maritime constructions, including boats, cargos, ferries, and ships. The comparably low strength of the 5xxx series Al-Mg alloys, however, restricts their use. Precipitation hardening will not strengthen this alloy because it is a non-heat-treatable alloy. The last strengthening procedures for this alloy include work hardening, dispersion strengthening, and grain-refinement strengthening. The creation of aluminium metal matrix composites (AMMCs) utilizing the dispersion strengthening effect is one of the most promising techniques for strengthening this type of Al-Mg alloy.

Aluminium metal matrix composites are significant contributions to the area of new materials. In comparison to regular alloys, AMMCs have very good mechanical properties and are easier to mould and fabricate into any shape or size. Increased strength, improved fatigue resistance, high corrosion resistance, high warmth resistance, and higher wear resistance are some of the crucial properties that composite materials possess [10]. According to the literature, adding reinforcements improves a variety of mechanical properties, including ultimate tensile strength [11–15], wear resistance, microhardness, elongation, etc. The ceramic particles that are evenly distributed throughout the fine-grain matrix of metal matrix composites are the reason for the improved mechanical properties [16–18]. These aluminium metal matrix composites are widely used in high-tech structural and functional applications, such as in the aircraft, mineral, defence, automobile, thermal management, marine, transportation, automotive, and sports and recreation areas [19–21].

Metal matrix composites (MMCs) are manufactured using a variety of manufacturing processes. Stirring casting, powder metallurgy, squeezing casting, in situ processes, deposition techniques, and electroplating are part of the manufacturing process used in the manufacture of AMMCs [22]. MMCs that use friction stir processing (FSP) have a distinct advantage over MMCs that use other manufacturing techniques. When opposed to most other strategies, FSP has several distinct benefits. FSP is a special processing method that was developed from friction stir welding (FSW) [23]. FSP is a solid-state method that improves the mechanical properties of the base material by homogenization, microstructural, and particle refinement [24]. FSP has been demonstrated to have a short route, homogeneity, accurate microstructure, and densification. FSP's benefits include a finer grain, processing zone homogeneity, densification, and the homogenization of the aluminium alloy and composite precipitates [25]. To develop a metal matrix composite using FSP, a groove or hole is formed in the base material and reinforcement particles are dispersed using a tool [23]. Numerous works have demonstrated that marine grades of aluminium can be reinforced with different reinforcements using FSP techniques. Al_2O_3 [26–28], TiC [27,28], TiO_2 [28,29], Al_3Ni [30], B_4C [31], SiC [32–35], are some of the reinforcements used to fabricate MMCS and some of the works developed with the different reinforcements will be discussed in detail in the following sections.

The literature has demonstrated that using various reinforcements in combination with the same base metal can result in different metal matrix composites with distinct properties. This review reports and compares the dominant base material from the marine-grade 5xxx series and reinforcements used in the fabrication of aluminium metal matrix composites suitable for marine grades produced using friction stir processing.

2. Review Available Literature

This literature gives information about the metal matrix composites fabricated with 5xxx series marine grades of aluminium using the FSP technique. The review was performed using 5xxx marine-grade aluminium alloys and different reinforcements.

2.1. AA5052-Based MMCs

Dolatkhah et al. [35] studied process factors concerning the mechanical properties and microstructure of an AA5052-SiC composite made by FSP. AMMC was created on the surface of 5052 aluminium sheets using FSP and 5-micrometre and 50-nanometre silicon carbide particles. Between passes, the impact of the traverse speed and rotational direction shifts was investigated. To determine the tool's rotational and traverse speeds that

produced the best powder dispersion, experiments were carried out utilizing all possible combinations of the three traverse speeds of 40 mm/min, 80 mm/min, and 125 mm/min and the three rotational speeds of 700 rpm, 1120 rpm, and 1400 rpm. Investigations were conducted on the impacts of tool rotational speed and particle size on the distribution of SiC particles, FSP passes, and the specimen's microstructure, wear, and microhardness characteristics. The findings indicate that the hardness and wear qualities were enhanced by increasing the number of passes, reducing the size of the SiC particles, and changing the tool's rotational motion between FSP passes. FSP and nano-sized SiC particles were used to produce an ultrafine microstructure. The use of SiC powder significantly improved the hardness. The microhardness increased by up to 55% over the parent material, and the rate of wear was reduced by 9.7 times.

Sharifitabar et al. [36] employed FSP to create an AA5052-Al_2O_3 nano-ceramic particle reinforced composite. After many FSP passes, the microstructural and mechanical characteristics of AA5052-Al_2O_3 surface composites were studied. FSP was conducted with varied tool-rotation speed to travel rate ratios (ω/υ) ranging from eight revolutions per minute to 100 revolutions per minute and a pin-tilting angle (φ) ranging from 2.5° to 5° to determine the best FSP conditions for the manufacture of stir zones without macroscopic faults. As the number of FSP passes increased, the stir zone's grain size decreased, and the surface composite created by four passes had a submicron mean grain size. The development of a nanocomposite with a mean cluster size of 70 nanometres after four passes and uniform Al_2O_3 particle dispersion in the base material were other benefits of increasing the FSP pass. Tensile testing showed that all FSP samples had more elongation than the base metal and that composites formed in three and four passes had greater UTS and yield strengths and lower elongation than FSPed materials prepared without powder under comparable conditions. Under good conditions, the four-pass composite's UTS and percentage elongation of the parental material increased to 118 and 165 percent, respectively.

Khodabakhshi et al. [37] created a high-strength ultra-fine-grained Al-Mg-SiC nanocomposite through a multi-step friction-stir-processing procedure. An ultra-fine-grained Al-matrix nanocomposite with improved tensile and indentation hardness was created using multi-pass FSP in this study. Using up to five cumulatively overlapping FSP operations, SiC nanoparticles of around 3.5 vol% were incorporated into an Al-Mg alloy matrix. Using scanning and electron backscattered electron microscopy, the nanoparticle dispersion in the stirred zone and their interfaces with the aluminium matrix were investigated. As a result of dynamic recrystallization during FSP, the grain and sub-grain structures of the SZ were refined to around 1.4 μm and less than 1 μm, respectively. The distribution and orientation of grains were considerably affected by the presence of SiC nanoparticles during FSP. Based on the Orowan looping and grain-refining processes, SiC nanoparticles showed both direct and indirect effects on the strengthening of the Al matrix. During FSP, the distribution and shape of the precipitates were partially dissolved. When compared to the base material, the processed UFGed nanocomposite increased hardness by up to 140%, yield stress by up to 75%, and ultimate tensile strength by up to 60%. A mixed ductile-brittle rupture behaviour was seen in the fractographic characteristics, with the ductile phase being more prominent and maintaining up to 30% of the nanocomposite elongation. A dislocation-based model was used to examine the tensile flow behaviour of the processed nanocomposite, and the results showed that grain boundary strengthening is the main mechanism at play.

Cao et al. [38] studied an AA5052-carbon-fibre composite's microstructural, tribological, and mechanical properties. The fabrication of carbon-fibre-reinforced AA5052 bulk composites using multi-pass FSP was successfully used in this work to enhance AA5052 wear resistance. According to microstructure tests, there was no apparent Al_4C_3 layer between the carbon fibres and the parent material in the composites, where they were uniformly distributed across a considerable volume. The composite's carbon-fibre orientation was random, due to the considerable plastic deformation caused by FSP. Further mechanical testing revealed that the hardness of the composite improved by 46.8 percent when compared to the parental metal, and the composite produced at 1000 revolutions per

minute and 75 mm per minute had an 18.6 percent higher UTS and a 13.0 percent greater elongation than the parental material. The wear tests demonstrated that the composite's wear process was more stable, with wear volume loss decreased by more than 70%. Carbon-fibre GNDs, fracture deflection, and load transfer have all been connected to enhanced mechanical properties.

Mathur et al. [39] investigated how titanium dioxide nano-particle reinforcement affected AA5052 using FSP. A 6-mm square pin tool was used with various parameters, such as a spindle rotational speed of 700 revolutions per minute, 1000 revolutions per minute, and 1300 revolutions per minute, as well as a traverse rate of 50 mm per minute, 65 mm per minute, and 80 mm per minute. At rotational and traverse speeds of 1000 mm per minute and 65 mm per minute, respectively, the maximum hardness value of 78 $\pm$ 1 Vickers hardness and tensile strength value of 193.1 $\pm$ 3 MPa were reached. The grain boundaries of the cast aluminium alloy 5052 were found to have micro-voids. Because of dynamic recrystallization generated by tool movement during the procedure, micro-voids were eliminated following friction stir processing. Because of dynamic recrystallization during the procedure, the grain size of the AMMCs decreased. Hardness was improved up to a 1000 rpm tool-rotating speed due to grain refinement and homogenous reinforcement distribution. However, after 1000 rpm, there was a decrease in hardness. According to the authors, excessive centrifugal force caused the reinforcement to be thrown away from the stir zone, resulting in a drop in hardness. During the specimen's tensile test, a ductile fracture was discovered.

2.2. AA5083-Based MMCs

Mishra et al. [40] is the founder of FSP-based composite production. In this investigation, composites were made using SiC as reinforcement and AA5083 alloy as the base material. They were successful in fabricating AA5083-SiC surface composites with various particle volume fractions. The surface of the AA5083 plates was cleaned before processing. A thin coating of silicon-carbide particles was formed on the surface of the plates by combining a small quantity of silicon-carbide powder with methanol. The process is the same as tape casting, with the exception that there is no binder in the mixture. After drying in air, the aluminium plates with a pre-applied SiC particle coating were exposed to FSP. The pin height of the tacking tool was 1.0 mm. The traverse rate and shoulder depth were changed while the tool was rotating at a constant speed of 300 rpm. To help with the forging process near the trailing edge of the shoulder, the tool spindle angle was fixed at 2.5°. The results of the investigation showed that the thickness of the surface composite layer ranged from 50 µm to 200 µm. The aluminium base material was uniformly coated with silicon-carbide particles. When reinforced with silicon carbide with a volume percentage of 27 and an average particle size of 0.7 µm, the surface composite has a microhardness of 173 HV, which is over twice that of the base material. The solid-state processing produced high-performance surface composites with very fine microstructures. In comparison to the base material, the microhardness and wear resistance were both 51% higher.

Zohoor et al. [41] used FSP to investigate the effect of processing variables on the formation of Al-Mg/copper composites. This work investigated the creation of an AA5083-copper surface composite layer employing aluminium alloy 5083 with copper particles by FSP. The FSP settings were 25 mm/min traverse speed, 750 rpm and 1900 rpm tool rotational speeds, and a tilt angle of 3°. The microstructure was analysed using SEM and optical microscopy. The effects of FSP pass numbers, rotational speed, and copper particle size on particle distribution patterns, microstructure, and microhardness were investigated. The samples containing micro- and nano-sized particles had small grains and a higher level of microhardness, according to the findings. In terms of tensile strength and ductility, the nano-sized particle composite outperformed the AA5083. To determine the phases present in the nugget zone, X-ray diffraction experiments were performed on specimens FSPed with Cu particles. Some reactions between the alloying elements are seen in XRD observations. After four passes using Cu-reinforcing particles, a considerable increase in

strength and hardness was noted. The chemical interaction between Cu particles and the aluminium material was also observed to increase with rotational speed.

Deepak et al. [42] studied the mechanical properties of an AA5083-SiC surface composite made via FSP. A CNC milling machine's spindle was configured to rotate at 1200 rpm with a machine bed traverse speed of 40 mm of the FSP tool. The findings demonstrated a considerable increase in the microhardness of the surface composite produced on the friction-stir-processed sample layer by doping AA5083 with hard SiC particles via FSP. The microhardness is highest in the middle of the FSPed zone at 155 HV and drops to roughly 84 HV at a distance of around 2 mm from the middle of the FSPed zone on each side. Despite its enhanced hardness, the FSPed sample had a worse wear resistance than AA5083. During wear testing, the FSPed sample had a higher friction force and a high coefficient of friction. This might be owing to the greater friction force and coefficient of friction reported during wear testing in the FSPed sample.

Bauri et al. [43] used FSP to examine how process variables and tool geometry affected the production of AA5083-Ni composites. First, a conventional cylindrical tool was utilized for FSP, and various processing parameters, including rotational and tool traverse rates, were studied to provide a defect-free nugget zone and uniform particle dispersion. To examine the impact of tool geometry, a different tool was employed with specific pin and shoulder characteristics. A traverse speed of 0.4 mm/s and a tool-rotation speed of 1200 rpm was found to be efficient for creating a stir zone free of defects. The dispersion of Ni particles was uniform for all parameters examined with the basic cylindrical tool, regardless of whether the stir zone was defective or not. It was found that the tool with spiral grooves on the shoulder and threads on the pin worked particularly well for both creating a sound stir zone and dispersing Ni particles. Ball-milled small particles were discovered to be more equally dispersed in the stir zone than coarse particles received as-is. Similar to this, FSP was used to reduce the aluminium base material's grain size from 25 microns to 3 microns. Equiaxed small grains with a high proportion of high-angle grain boundaries and a narrow range of grain sizes made up the microstructure. The impact of particle addition on the mechanical properties of the alloy was also investigated. The composite's strength significantly increased as compared to the base material, and it also acquired a high level of ductility.

Hossieni et al. [44] fabricated AA5083 surface composites reinforced with CNTs and cerium oxide nanoparticles via FSP. To fabricate a surface-reinforced composite, MWCNT and nanosized cerium-oxide particles were combined with the AA5083 base material by FSP. Both separately and in combination, the effects of different nanosized reinforcements on the microstructure, corrosion resistance, and mechanical characteristics of FSPed surface composites were examined. With travel rates of 35 mm/min and 45 mm/min, rotation speeds of 600 rpm and 800 rpm, and a tilt angle of 5°, a threaded cylindrical hardened steel technique was used. FSPed samples were put to the test and compared to the parent material in terms of mechanical properties and corrosion resistance. The highest tensile strength and hardness were attained by the hybrid composite of cerium oxide and carbon nanotubes, which had a volume ratio of 75:25. Cerium oxide alone significantly improved the base material's resistance to pitting. Potential dynamic polarization tests were used to analyse the samples' corrosion behaviour in terms of passivation range and pitting potential. Microstructural investigation using optical and electron microscopes demonstrated that reinforcements were evenly distributed across the stir zone and that substantial grain refinement occurred. The mechanical properties of produced composites incorporating cerium oxides or CNTs were enhanced. The hybrid composite with 75 percent carbon nanotubes and 25 percent cerium oxide exhibited the best properties. The hardness was 118 percent greater and the UTS was 42 percent higher than the parent aluminium alloy. Grain refinement improved reinforcement distribution, and microstructural modification is achievable in SZ.

Kumar et al. [45] investigated the effect of ball milling and particle size on the surface composite FSPed AA5083-Ni. To make a metal-particle-reinforced composite, FSP was

employed to integrate Ni particles into AA5083 material. To achieve a flawless nugget zone and uniform particle distribution, a range of rotation rates tools from 1000 revolutions per minute to 1800 revolutions per minute and a range of traverse rates from 6 mm per minute to 24 mm per minute were investigated. Results showed that finer particles of 10 µm for the ball-milled sample were dispersed more consistently in the composite than in the base material during the modification of process parameters for uniform particle distribution. Before being included in the AA5083, the particles were ball-milled. A thin intermetallic layer was created by the more finely dispersed ball-milled particles. An AA5083-Ni composite intermetallic was found in the layer. The processed composite did not contain this layer when tiny particles of a similar size (10 µm) were merged using the same FSP parameters. The outcomes showed that particle ball milling enhanced the composite's microstructure. The ball-milled particle is in a high-energy state because of the interfacial layer formation. In terms of strength, both composites performed better than the unreinforced AA5083. Additionally, FSP reduced the base material's grain size from 25 to 3.5 µm, resulting in a stronger composite. The strength and ductility of the ball-milled composite with the small Ni particles as received were less than anticipated due to the existence of the interfacial reaction layer.

Yuvaraj et al. [46] used FSP to create an AA5083-B_4C nanocomposite and tribologically characterize it. FSP was used to produce an AA5083 incorporated with boron carbide as a reinforced layer. As reinforcements, nano-sized and micro-sized B_4C particles were utilized. Optical microscopy and SEM examinations were used to examine the FSPed surface composite layer. To produce surface composites using FSP, it is important to consider the amount of reinforcement and the number of passes. Before manufacturing, several tests were carried out, and it was found that the constant rotational and transverse speeds were, respectively, 1000 revolutions per minute and 25 mm per minute. Microhardness and tensile tests were used to assess the FSPed surface composite's mechanical characteristics. The outcomes were compared with the base metal's properties. The effects of reinforcement and the number of passes on properties were investigated. To assess the tribological performance of the surface composite, the pin-on-disk test was run. In terms of wear resistance, tensile behaviour, and hardness, the surface composite layer produced in three passes with nanoparticle reinforcement performed better than the base metal. The dispersion of nanoparticles in the base material became more uniform compared to a single-pass FSP nanocomposite, resulting in increased hardness. After three passes, the microhardness of the nanocomposite was raised to 122 Hv. The hard B_4C particles placed on the surface of the AA5083 improved the wear resistance of the nanocomposite. When compared to non-reinforced samples, the one-pass approach resulted in significant reductions in yield and UTS values of surface composites. Despite this, the surface composite's microhardness was shown to be larger than that of the unreinforced samples, and the wear rate was also lowered.

Kumar et al. [47] studied the wear properties of an AA5083-tungsten composite made using the FSP technique. To create metal-particle-reinforced surface composites, FSP was employed to integrate tungsten particles in an AA5083 material. On an AA5083 plate with a thickness of 10 mm, a groove of 60 × 2 × 1.5 mm was created. Ten-micrometre tungsten particles were maintained in the groove. The FSP tool rotated at 1200 revolutions per minute and had a transverse speed of 24 mm. Wear test samples with a diameter of 8 mm and a height of 10 mm were cut using EDM. The results demonstrated that the microstructure had a homogeneous distribution. The particles were evenly distributed in the base material, and the grain size was refined using FSP. The tungsten particles remained elemental after X-ray diffraction, and an additional investigation did not find an intermetallic peak. The composite surface layer outperformed the base and FSPed alloys in terms of wear resistance. The base and FSPed sample's worn surface inspections revealed that the composite exhibits mild and adhesive oxidative wear at all three loads, transitioning to severe abrasive and delamination-type wear at higher loads.

Khan et al. [48] examined the cold formability of boron-carbide particles and carbon nanotubes in friction-stir-processed aluminium composites. The base materials AA5083 and MWCNTs, as well as B_4C reinforcements, were used. The bend-ductility test was used to assess the cold formability of FSPed aluminium metal matrix composites. Carbon-nanotube-containing composites fractured under bending, whereas boron-carbide-containing composites survived; hybrid composites cracked, but the crack was less than nanotube-only composites. Poor interfacial nanotube or aluminium bonding and insufficient nanotube dispersion are two possible explanations. The cold formability of the composites is determined by their mechanical and microstructural properties. The B_4C-reinforced composite increased tensile strength and hardness by 28 percent and passed the bend ductility test with no surface cracks. The MWCNT-composite reduced fracture strain by 50% while also improving the hardness and tensile properties. The bend-ductility test reveals fractures caused by the CNT clusters that developed in the TMAZ, since it is a single pass FSP. While fracture strain was decreased by 16%, tensile strength and hardness were also increased by 10% and 5%, respectively. This specimen failed the bend-ductility test due to weak MWCNT and aluminium alloy interfacial bonding and insufficient MWCNT dispersion in the composite.

Mirjavadi et al. [49] studied the wear and mechanical properties of an AA5083-ZrO_2 composite made using FSP. Multi-pass FSP with zirconia nanoparticles was used to fabricate surface nanocomposites on AA5083 sheets in this investigation. The specimen's microhardness, microstructure, wear parameters, and tensile strength were all studied with the number of passes. Following many trial and test runs, it was determined that a traverse speed of 50 mm/min and a rotation rate of 800 rpm, which was also similar to reference [50], was the most suited in terms of possible flaws. These rates were utilized for all FSP passes. For all samples, the tool tilt angle concerning the workpieces was around 3°. As a result, it was discovered that FSP iteration consistently increases the material's tensile strength and microhardness. This was primarily brought about by the FSP-enhanced microstructural modification, which included better powder dispersion, smaller grains, and fewer clustered particles. The eight-pass friction stir processed nanocomposite was subjected to EBSD and TEM examination, which revealed a large number of high-angle grain boundaries as well as ongoing dynamic recrystallization. Wear tests showed that the further processed sample's wear rate was much lower than that of the base material. Furthermore, the fracture surface of the eight-pass treated material, such as the base material, showed ductile fracture with dimples and voids. With a microhardness of 140 Vickers, the composite with eight passes had the most grain-refined structure. In addition, the wear rate of composites generated in eight passes was lowered.

Khan et al. [51] used FSP to evaluate the impact of FSP spacing on the growth of B_4C- and MWCNT-reinforced AA5083 composite. In this work, FSP was used to add boron carbide and carbon nanotube particles into AA5083 to create hybrid surface composites. Using a single-pass approach, the impact of metal loss in cavities made to contain reinforcements at 8- and 10-mm inter-cavity spacings were examined. A single pass of FSP was run at a 2° tilt angle, 16 mm/min traverse speed, and 750 rpm rotating speed to prepare surface composites. Surface composites with individually reinforced B_4C and MWCNT particles, as well as a hybrid composite with both reinforcements, were created. Microstructural analysis and an examination for the existence of any flaws were carried out using optical microscopy and SEM. Mechanical tests found that composites with 10-millimetre inter-cavity spacing and boron-carbide particles increased their UTS and microhardness by up to 38% and 18%, respectively. The cold formability of FSPed composites was then evaluated using the U-bend ductility test. Due to severe cracking brought on by clustering and insufficient material-loss compensation, carbon nanotube composites with an inter-cavity spacing of 8 mm failed. This had a substantial influence on the ultimate mechanical properties. To compensate for material loss, it was determined that sinking reinforcement in the parental material was required. It was observed that if the material loss in the form of a cavity for reinforcements is not compensated for, a higher empty volume leads to a decrease

in mechanical properties. A 10 mm inter-cavity spacing made it possible to achieve the greatest reinforcement sinking and the smallest amount of clustering when using carbon nanotubes in single-pass friction stir processing.

Jain et al. [52] looked at the mechanical characteristics, sliding wear behaviour, and microstructure when fabricating AA5083-B_4C/SiC/TiC surface composites using FSP. In this investigation, FSP was used to produce three distinct AA5083 surface composites reinforced with TiC, B_4C, and SiC particles. Three sequential FSP passes and the mechanical properties of reinforced particles were studied. A tool tilt angle of 3°, a transverse rate of 25 mm/min, several passes, and a rotating speed of 1600 rpm were selected based on experimental tests to provide a sound FSP area and homogenous particle dispersion in the stirred zone. The FSPed sample's mechanical properties were assessed and compared to the parental material. With dense particulate distribution on both the advancing and retreating sides of the stir region, as well as particle-free zones and strong particle-matrix bonding in some places, the microstructure revealed substantial grain refinement. FSP induces significant plastic deformation in the materials, allowing the constituent phase to mix and refine. The FSPed sample's wear resistance was assessed and compared to the parental material. The inclusion of TiC, B_4C, and silicon carbide particles in the parental material (AA5083) improves wear properties, according to the findings. The findings showed that the wear mode changed from abrasive to delamination when a pin-on-disc tribometer was used to examine the wear mechanism. Furthermore, the findings show that adding TiC, B_4C, and SiC particles to the parental material improves the tensile properties while also enhancing its hardness. The fracture mode of SiC- and TiC-particle-reinforced surface composites was found to be ductile, whereas the fracture mode of B_4C reinforced surface composites was found to be bimodal. When compared to the AA5083-SiC/TiC composite, the UTS and microhardness of the AA5083-B_4C composite were 349 MPa and 132.56 ± 2.52 Hv, respectively. The AA5083-B_4C composite has a minimum wear rate of 18×10^{-5} mm^3/Nm.

Owa and Shimizu [53] used FSP to investigate the production and strength behaviour of an MWCNT-reinforced AA5083 composite. MWCNTs were included in AA5083 through FSP to boost the strength of the alloy, which is used in a range of industries. The FSP approach was used to successfully produce the AA5083-MWCNT composites. In comparison to the base material, the composite grain size was improved greatly. The composites have no voids or other faults under FSP-optimized settings. The grain refining and uniform distribution of MWCNTs were accomplished due to a composite powder composed of MWCNTs and AA5083. While the UTS increased from 13 to 16 percent, the proof stresses of the composite ranged from 53 to 61 percent higher than those of the base material.

Jain et al. [54] employed friction stir processing to develop and analyse AA5083-CNTs/SiC composites. To make hybrid and mono composites, AA5083 base material was reinforced with CNT and micron-sized SiC particles by FSP. In both individual and aggregate forms, the impact of CNTs/SiC on the texture, mechanical properties, and microstructural development texture of FSPed AA5083 composites was examined. All of the samples were subjected to three passes of homogeneous reinforcement dispersion at a transverse speed of 20 mm/min and a rotating speed of 1600 rpm. For comparison, FSP was performed on a parental material without reinforcement under similar experimental conditions. After dynamic recrystallization, TEM and EBSD investigations showed a dislocation rearranged to create high-angle grain boundaries, and equiaxed recrystallized microstructure, respectively. Multiple passes resulted in a generally poor texture intensity over the stir zone of FSPed samples. By incorporating carbon-nanotube/silicon-carbide particles into the AA5083 base material, the Zener–Holloman and particle-stimulated nucleation mechanisms were activated, resulting in the formation of randomly oriented grains. Silicon-carbide particles are uniformly disseminated with good interfacial bonding in FSPed composites, and carbon nanotubes are partly reacted with an AA5083 material to generate an in situ Al_4C_3 intermetallic compound. The maximal UTS of the AA5083-CNTs/SiC hybrid composite is 361 Mpa, while the tensile strength of the base material is 298 Mpa. On the fracture surface of the SiC-reinforced composite, the voids initiating at the matrix–particle

interface areas were observed. Hardness testing revealed that AA5083/SiCasSiCs had the highest difference in hardness, 1.5 times that of the base material. AA5083/SiCasSiCs also had a greater hardness and elastic modulus. The hybrid composite increases hardness by 1.4 times.

Naghshekesh et al. [55] evaluated the influence of FSP on the surface of AA5083 using graphene oxide as a reinforcing material. A surface nanocomposite formed of graphene oxide was created utilizing FSP in a liquid-cooled condition to enhance the AA5083's microstructural and mechanical properties. To accomplish this, FSP was employed to do up to three passes on a parental material with and without reinforcing particles. The friction-stir-processed AA5083, the base material, and the resulting surface nanocomposite's microstructural and mechanical properties were examined. With the use of electron backscatter diffraction, the microstructure was examined. After processing, the nanocomposite's grain size was found to be around 1 μm. The base material's grain size was 23 ± 2.3 μm, but the specimen's grain size without reinforcement was 6 ± 1.1 μm. This discrepancy was mostly caused by the considerable impact of the reinforcing particles on grain formation in the nanocomposite specimen. According to research on the mechanical properties of the parental material, nanocomposite, and FSPed specimen, applying a cooling environment while performing the procedure increases the microhardness of the stir zone in comparison to the parental material. In the presence of graphene oxide particles, the microhardness increased to 123 1.7 HV. In terms of tensile properties, the nanocomposite performed better than the parent material and the FSPed sample.

Prabhakar et al. [56] created AA5083-CNT composites by friction stir processing to study the effects of grain refinement and carbon nanotubes on corrosion and mechanical properties. FSP dispersed CNT into AA5083 to create a metal matrix composite in the current study. In the stir zone, microstructural investigations indicated smaller grains and nonuniform CNT dispersion. The small grains and presence of CNT in the composite led to a 25% improvement in hardness when compared to unprocessed aluminium alloy, which is connected to the fine grains and presence of CNT in the composite. According to the electrochemical tests, the FSPed composite showed a somewhat higher corrosion resistance. The findings reveal that the addition of CNT, in combination with the grain size effect, has a considerable impact on the corrosion resistance of AA5083. Based on the findings, it can be concluded that adding CNT to AA5083 through FSP can increase mechanical performance. However, care must be taken to enhance CNT dispersion, since the presence of CNT has a significant impact on corrosion resistance. It was discovered that employing FSP to produce AA5083-CNT composites allows for the construction of lightweight energy-efficient structures with high mechanical properties and corrosion resistance.

Papantoniou et al. [57] studied a new friction-stir-process technique for the hardening and surface modification of aluminium alloys: AA5083-Cu. In this study, FSP was performed on thick AA5083 plates. A pure copper sheet with a 4-mm-by-0.8-mm cross-section was friction stir processed into a machining groove on the top side of the aluminium plate. Each sample was produced using one, two, or three FSP passes. The effects of the AA5083/Cu composite on metallurgy and mechanical were then investigated. The findings show that the Cu thin sheet was successfully incorporated into the AA5083 nugget zone, with non-integrated Cu disappearing after many FSP passes. The reinforcement was divided into small particles, blended, and spread throughout the SZ. There were various intermetallic phases detected after FSP overlapping, as well as the particles dimensionally concerned in the material flow direction because of the rotating action. The interplanar diffusion-interfacial migration phenomenon resulted in Cu particles becoming enriched with aluminium atoms due to the severe plastic deformation brought on by heat production and material movement close to the tool. XRD has proposed the fabrication of intermetallics such as Al_2Cu, $AlCu_4$, and $MgCu_2$. Cu diffusion and the production of diverse hard intermetallics increased the hardness of the surface composite. Almost all of the Cu was incorporated into the nugget region as the FSP passes were increased, primarily as Cu-based micron-sized intermetallic particles and secondarily by Cu diffusion in the

AA5083 material. The microhardness inside the nugget zone rose from 77 HV to 138 HV due to the presence of complex intermetallic compounds created by the high heat input and strong plastic deformation.

3. Results and Summary

3.1. Results

Table 1 summarizes the metal matrix composites fabricated from the 5xxx series of aluminium magnesium alloys using only marine grades reinforced with various reinforcements using the FSP process. The literature study reveals that SiC particles are the most frequent type of reinforcement that has been employed to develop composites.

Table 1. Aluminium metal matrix composites fabricated from the 5xxx series of aluminium magnesium alloys using only marine grades reinforced with various reinforcements using the FSP process.

Reference	Base Material	Reinforcement	Outcome
[35]	AA5052	SiC	The results showed a 55% increase in hardness value and a 9.7 times greater wear resistance than the AA5052 base material.
[37]	Al5052	SiC	Hardness, yield strength, and UTS improved by 140, 60, and 75%, respectively.
[39]	AA5052	TiO_2	At tool rotational speed and traverse speed of 1000 RPM and 65 mm/min, respectively, the maximum hardness and tensile strength values (78 $\pm$ 1 Hv and 193.1 $\pm$ 3 Mpa) were achieved. The grain boundaries of the cast AA5052 were found to have micro-voids. The specimen's tensile test revealed the ductile fracture. There were no defects discovered in the FSPed zone.
[58]	AA5052-H32	TiO_2, MgO and Al_3Ti	Particles of Al_3Ti and MgO (50 nm) were detected. The composite showed 90% HAGBs and a grain size of 2 mm. At higher test temperatures, the composite's deformation activation energy was discovered to be 456 kJ/mol.
[59]	AA5052-H32	TiO_2	The processing zone contains particles of Al_3Ti and MgO. Pre-treatment decreased strain hardening and strain rate sensitivity. Annealed and wrought FSPed samples had microhardness of 87.9 $\pm$ 2 and 82.4 $\pm$ 1.6 Hv, respectively.
[60]	AA5052-H32	TiO_2	In a 2-mm fine-grained matrix, nanoscale Al_3Ti, and MgO phases may be found. At high TiO_2 content (3.5 vol%) and 6 FSP passes, a greater yield strength of 158 Mpa, an ultimate tensile strength of 252 Mpa, and an elastic modulus of 85 Gpa were recorded. With six FSP passes, the endurance limit of 154 and 148 Mpa was recorded at 2 and 3.5% of the TiO_2 volume percent.
[61]	AA 5052	GNPs	AMMCs' improved mechanical characteristics
[62]	5052	ZrO_2	The coefficient of friction (COF) was reduced with an increase in rotational speed during FSP of the ZrO_2 reinforced sample, increasing the wear resistance of aluminium alloy 5052 to 36.8%.
[63]	Al 5052	SiO_2	SiO_2 homogenous dispersion was accomplished.
[40]	AA 5083	SiC	A well-distributed, 50–200-lm thick AA5083/SiC surface composite layer with an excellent bonding matrix was created. The surface composite AA5083/27 vol% SiC has a microhardness of almost twice as much as the AA5083 base material.
[42]	AA5083	Cu	The best powder dispersion was reportedly obtained with a four FSP-pass count.
[46]	AA5083	B_4C	In the one-pass method, there were some visible reductions in the yield and ultimate tensile strength values of surface composites when compared to the non-reinforced samples. Despite this, it was shown that the surface composite microhardness was greater than that of the non-reinforced samples, and their wear rate was also lower.
[51]	Al 5083	MWCNT	Tensile strength and hardness both increased by 38 and 18%, respectively.

Table 1. *Cont.*

Reference	Base Material	Reinforcement	Outcome
[56]	Al5083	CNT	Microstructural analysis showed smaller granules and non-uniform CNT dispersion in the stir zone. According to microhardness studies, the tiny grains and presence of CNT in the composite led to a hardness increase of up to 25% when compared to unprocessed Al alloy. Electrochemical experiments revealed that an FSPed composite has somewhat greater corrosion resistance.
[57]	AA5083	Cu	The XRD suggested that intermetallic compounds such $AlCu_4$, Al_2Cu, and $MgCu_2$ formed. The improvement in surface composite hardness was induced by the diffusion of copper and the development of different hard intermetallic. The copper-reinforced stir zone microhardness distribution increased significantly from 77 HV to 138 HV.
[64]	AA5083	SiC, Al_2O_3 and SiC/Al_2O_3	The findings indicated that the addition of more ceramic particles raised the composite's average hardness by 30%. As ceramic powder SiC reinforcement was added this enhanced the wear resistance of AA5083-SiC by 40%. At two FSP passes, the composites containing 50% Al_2O_3 and 50% SiC had the maximum hardness.
[65]	AA5083	Hybrid Reinforcement	There was intermetallic formation. Intermetallic phase development increased the composite's hardness and wear resistance.
[66]	AA5083	CNT + Al_2O_3	CNT's presence facilitated work hardening. The presence of CNT/Al_2O_3 limits the dislocation movement, improving the metal matrix's hardness in the process.
[67]	Al5083	CeO_2 and SiC	CeO_2 and SiC, at the perfect volume ratio of 75:25, were shown to have improved mechanical and corrosion properties for the composite. Al5083-SiC (25%)-CeO_2 (75%), a hybrid composite, was shown to have the best mechanical and corrosion properties.
[68]	Al5083	B_4C/TiC	Decreased wear rate for the hybrid Al5083-B_4C/TiC composite was observed.
[69]	Al5083	SiC and MoS_2	Improved wear properties for Al5083 hybrid composites distributed with SiC and MoS_2 were obtained.
[70]	AA5083	SiC, ZrO_2, and Gr	SiC, ZrO_2, and Gr particles were incorporated into the AA5083 alloy as reinforcement and used to increase the ultimate strength since the hybrid ratio of the reinforcement particles greatly altered the mechanical characteristics.
[71]	AA5083	Sic	The FSP-processed composite's maximum micro-hardness and tensile strength were determined to be 1.75 Gpa and 78 Mpa, respectively.

3.2. Summary

This review's main objective was to take into account the work that has been performed regarding the fabrication of AMMCs using the 5xxx series of aluminium magnesium alloys using only marine grades. The goal was to determine which reinforcement and base material are employed the most in the fabrication of AMMCs. According to the reviewed literature, AA5083 is the base material that is most frequently used to fabricate AMMCs using the FSP approach (see Figure 1). The fabrication of an AMMCs employing FSP, friction stir additive, and FSW has only been tried once with AA5059. The only base alloys that have not been used to make AMMCs using the FSP approach or any other method for fabricating a composite are AA5386, AA5436, and AA5454. The use of different reinforcements on various base materials is also shown in Figure 2, with SiC particles, CNTs, B_4C, and TiO_2 appearing to be the most commonly used reinforcements. As this study shows, there is less research on aluminium metal matrix composites fabricated using coal as reinforcements; thus, it will be beneficial for future studies to follow this direction.

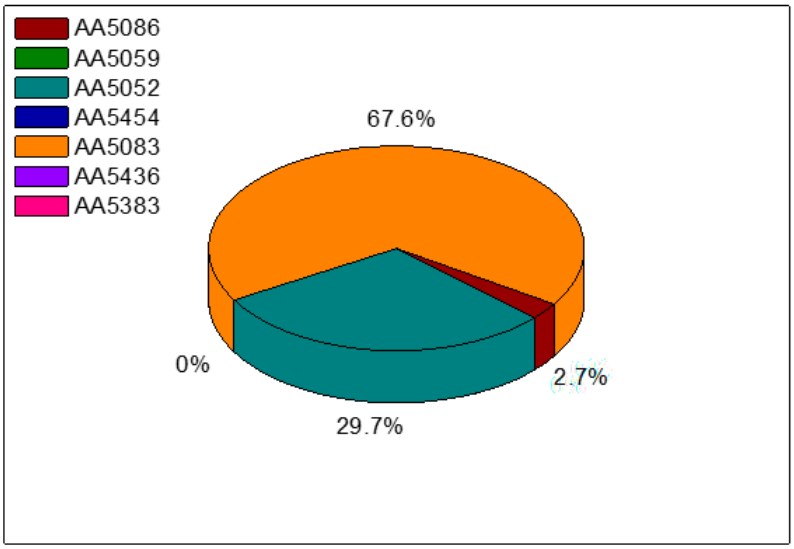


Figure 1. Base material used to fabricate AAMMCS using 5xxx series marine grade.

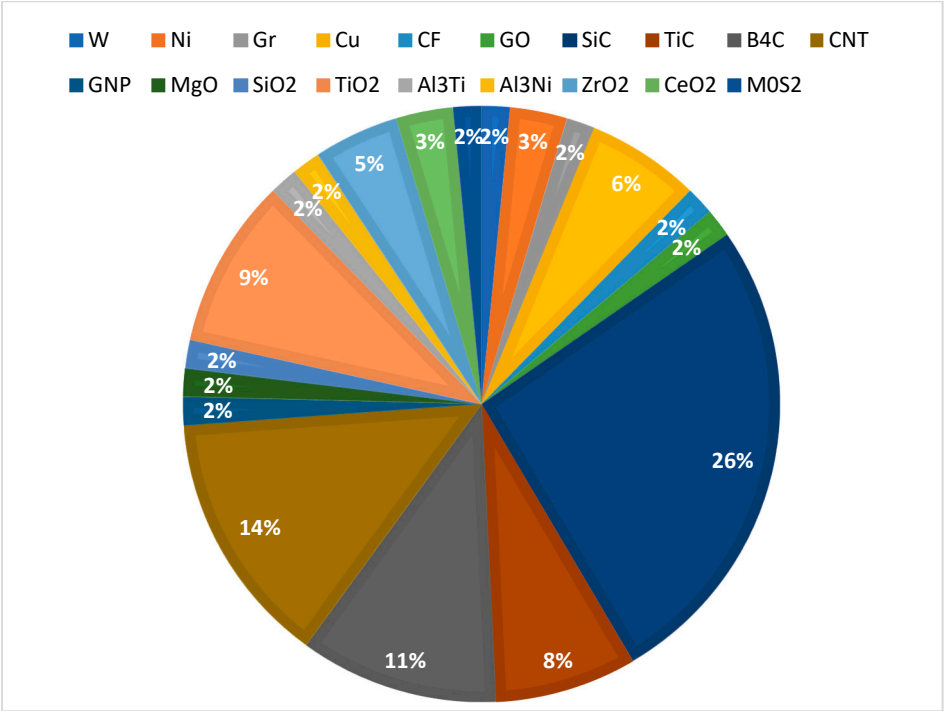


Figure 2. Graphical representation of reinforcement usage on different base materials.

4. Conclusions

The development of AMMCs suitable for the marine field is still a work in progress. Most MMC investigations achieve AMMC precipitate grain refinement, treated zone homogeneity, densification, and homogenization. AMMCs are undeniably capable of exhibiting refined grains, superior damping, strength, wear, enhanced hardness, and reduced thermal expansion, making them appropriate for a wide range of applications. This part of the work examines the impact of reinforcing particles, process parameters, multiple passes, and active cooling on mechanical characteristics during the fabrication of 5000-series AMMCs using FSP. This paper reports on the available literature on aluminium metal matrix composites fabricated with 5xxx-series marine-grade aluminium alloy using FSP.

Author Contributions: Conceptualization, V.M.; methodology, S.M.; validation, O.M., V.M. and S.M.; formal analysis, S.M.; investigation, O.M.; resources, V.M.; data curation, S.M. and O.M.; writing—original draft, O.M.; writing—review and editing, S.M. and V.M.; visualization, O.M.; supervision, V.M. and S.M.; project administration, V.M. All authors have read and agreed to the published version of the manuscript.

Funding: This research received no external funding.

Data Availability Statement: Not applicable.

Acknowledgments: The authors would like to thank the Cape Peninsula University of Technology for providing them with unrestricted access to the equipment required for the study.

Conflicts of Interest: The authors declare no conflict of interest.

References

1. Starke, E.A., Jr.; Rashed, H.M.M.A. *Alloys: Aluminium*; Elsevier: Amsterdam, The Netherlands, 2017.
2. Sielski, R.A. Research needs in aluminium structure. *Ships Offshore Struct.* **2008**, *3*, 57–65. [CrossRef]
3. Lamb, T.; Beavers, N.; Ingram, T.; Schmieman, A. The benefits and cost impact of aluminium naval ship structure. *J. Ship Prod. Des.* **2011**, *27*, 5–49. [CrossRef]
4. Altenburg, C.J.; Scott, R.J. *Design Considerations for Aluminium Hull Structures-Study of Aluminium Bulk Carrier*; Gibbs & Cox Inc.: New York, NY, USA, 1971.
5. Yazdipour, A.; Dehghani, K. Modeling the microstructural evolution and effect of cooling rate on the nanograins formed during the friction stir processing of Al5083. *Mater. Sci. Eng. A* **2009**, *527*, 192–197. [CrossRef]
6. Vijayan, S.; Raju, R.; Rao, S.R.K. Multiobjective optimization of friction stir welding process parameters on aluminum alloy AA 5083 using Taguchi-based grey relation analysis. *Mater. Manuf. Process.* **2010**, *25*, 1206–1212. [CrossRef]
7. El-Danaf, E.A.; El-Rayes, M.M.; Soliman, M.S. Friction stir processing: An effective technique to refine grain structure and enhance ductility. *Mater. Des.* **2010**, *31*, 1231–1236. [CrossRef]
8. Ertuğ, B.; Kumruoğlu, L.C. 5083 type Al-Mg and 6082 type Al-Mg-Si alloys for ship building. *Am. J. Eng. Res.* **2015**, *4*, 146–150.
9. Nik, W.W.; Sulaiman, O.; Fadhli, A.; Rosliza, R. Corrosion behaviour of aluminium alloy in seawater. *Proc. MARTEC* **2010**, 175–180.
10. Srivastava, A.K. Statistical optimization of wire-edm during the processing of hybrid mmc. *Int. J. Mech. Prod. Eng. Res. Dev.* **2018**, *8*, 783–792.
11. Davis, L.C.; Allison, J.E. Residual stresses and their effects on deformation. *Metall. Trans. A* **1993**, *24*, 2487–2496. [CrossRef]
12. Chawla, N.; Shen, Y.L. Mechanical behavior of particle reinforced metal matrix composites. *Adv. Eng. Mater.* **2001**, *3*, 357–370. [CrossRef]
13. Bauri, R.; Yadav, D.; Kumar, C.S.; Balaji, B. Tungsten particle reinforced Al 5083 composite with high strength and ductility. *Mater. Sci. Eng. A* **2015**, *620*, 67–75. [CrossRef]
14. Kumar, N.; Gautam, R.K.; Mohan, S. In-situ development of ZrB2 particles and their effect on microstructure and mechanical properties of AA5052 metal-matrix composites. *Mater. Des.* **2015**, *80*, 129–136. [CrossRef]
15. Huang, G.; Shen, Y. The effects of processing environments on the microstructure and mechanical properties of the Ti/5083Al composites produced by friction stir processing. *J. Manuf. Process.* **2017**, *30*, 361–373. [CrossRef]
16. Onat, A. Mechanical and dry sliding wear properties of silicon carbide particulate reinforced aluminium–copper alloy matrix composites produced by direct squeeze casting method. *J. Alloy. Compd.* **2010**, *489*, 119–124. [CrossRef]
17. Alizadeh, M.; Paydar, M.H. Fabrication of Al/SiCP composite strips by repeated roll-bonding (RRB) process. *J. Alloy. Compd.* **2009**, *477*, 811–816. [CrossRef]
18. Ramachandra, M.; Radhakrishna, K. Effect of reinforcement of flyash on sliding wear, slurry erosive wear and corrosive behavior of aluminium matrix composite. *Wear* **2007**, *262*, 1450–1462. [CrossRef]
19. Rambabu, P.P.N.K.V.; Eswara Prasad, N.; Kutumbarao, V.V.; Wanhill, R.J.H. Aluminium alloys for aerospace applications. *Aerosp. Mater. Mater. Technol.* **2017**, 29–52.
20. Suryanarayana, C.; Al-Aqeeli, N. Mechanically alloyed nanocomposites. *Prog. Mater. Sci.* **2013**, *58*, 383–502. [CrossRef]
21. Casati, R.; Vedani, M. Metal matrix composites reinforced by nano-particles—A review. *Metals* **2014**, *4*, 65–83. [CrossRef]
22. Ramnath, B.V.; Elanchezhian, C.; Annamalai, R.M.; Aravind, S.; Atreya, T.S.A.; Vignesh, V.; Subramanian, C. Aluminium metal matrix composites—A review. *Rev. Adv. Mater. Sci.* **2014**, *38*, 55–60.
23. Sudhakar, M.; Srinivasa Rao, C.H.; Meera Saheb, K. Production of Surface Composites by Friction Stir Processing. *Mater. Today Proc.* **2018**, *5*, 929–935. [CrossRef]
24. Mironov, S.; Sato, Y.S.; Kokawa, H. Friction-stir welding and processing of Ti-6Al-4V titanium alloy: A review. *J. Mater. Sci. Technol.* **2018**, *34*, 58–72. [CrossRef]
25. Sanusi, K.O.; Akinlabi, E.T. Friction-stir processing of a composite aluminium alloy (AA 1050) reinforced with titanium carbide powder. *Mater. Tehnol.* **2017**, *51*, 427–435. [CrossRef]

26. Mohamed, S.S. Microstructure and mechanical properties of AA2024/Al_2O_3 surface nanocomposites fabricated using friction stir processing. *Eng. Res. J.* **2018**, *1*, 1–6.
27. Thangarasu, A.; Murugan, N.; Dinaharan, I. Microstructure and microhardness of AA1050s/TiC surface. *Sadhana* **2012**, *37*, 579–586. [CrossRef]
28. Beygi, R.; Mehrizi, M.Z.; Eisaabadi, B.G. Friction stir processing of al with mechanically alloyed Al-TiO_2-graphite powder: Microstructure and mechanical properties. *J. Mater. Eng. Perform.* **2017**, *26*, 1455–1462. [CrossRef]
29. Gudla, V.C.; Jensen, F.; Simar, A.; Shabadi, R.; Ambat, R. Friction stir processed $AlTiO_2$ surface composites: Anodising behaviour and optical appearance. *Appl. Surf. Sci* **2015**, *324*, 554–562. [CrossRef]
30. Shahi, A.; Sohi, M.H.; Ahmadkhaniha, D.; Ghambari, M. In situ formation of Al–Al_3Ni composites on commercially pure aluminium by friction stir processing. *Int. J. Adv. Manuf. Technol.* **2014**, *75*, 1331–1337. [CrossRef]
31. Rana, H.G.; Badheka, V.J.; Kumar, A. Fabrication of Al7075/B4C surface composite by novel friction stir processing (FSP) and investigation on wear properties. *Procedia Technol.* **2016**, *23*, 519–528. [CrossRef]
32. Srivastava, M.; Siddiquee, A.N.; Rathee, S.; Maheshwari, S. Optimisation of friction stir processing parameters to fabricate AA6063/SiC surface composites using Taguchi technique. *Int. J. Mater. Prod. Technol.* **2019**, *58*, 16. [CrossRef]
33. Rathee, S.; Maheshwari, S.; Siddiquee, A.N.; Srivastava, M. Investigating effects of groove dimensions on microstructure and mechanical properties of AA6063/SiC surface composites produced by friction stir processing. *Trans. Indian Inst. Met.* **2017**, *70*, 809–816. [CrossRef]
34. Tang, J.; Shen, Y.; Li, J. Influences of friction stir processing parameters on microstructure and mechanical properties of SiC/Al composites fabricated by multi-pin tool. *J. Manuf. Process.* **2019**, *38*, 279–289. [CrossRef]
35. Dolatkhah, A.; Golbabaei, P.; Givi, M.B.; Molaiekiya, F. Investigating effects of process parameters on microstructural and mechanical properties of Al5052/SiC metal matrix composite fabricated via friction stir processing. *Mater. Des.* **2012**, *37*, 458–464. [CrossRef]
36. Sharifitabar, M.; Sarani, A.; Khorshahian, S.; Afarani, M.S. Fabrication of 5052Al/Al_2O_3 nanoceramic particle reinforced composite via friction stir processing route. *Mater. Des.* **2011**, *32*, 4164–4172. [CrossRef]
37. Khodabakhshi, F.; Gerlich, A.P.; Švec, P. Fabrication of a high-strength ultra-fine-grained Al-Mg-SiC nanocomposite by multi-step friction-stir processing. *Mater. Sci. Eng. A* **2017**, *698*, 313–325. [CrossRef]
38. Cao, X.; Shi, Q.; Liu, D.; Feng, Z.; Liu, Q.; Chen, G. Fabrication of in situ carbon fiber/aluminium composites via friction stir processing: Evaluation of microstructural, mechanical, and tribological behaviors. *Compos. Part B Eng.* **2018**, *139*, 97–105. [CrossRef]
39. Mathur, V.; Patel, G.C.M.; Shettigar, A.K. Reinforcement of titanium dioxide nanoparticles in aluminium alloy AA 5052 through friction stir process. *Adv. Mater. Process. Technol.* **2019**, *5*, 329–337. [CrossRef]
40. Mishra, R.S.; Ma, Z.Y.; Charit, I. Friction stir processing: A novel technique for fabrication of surface composite. *Mater. Sci. Eng. A* **2003**, *341*, 307–310. [CrossRef]
41. Zohoor, M.; Givi, M.B.; Salami, P. Effect of processing parameters on the fabrication of Al-Mg/Cu composites via friction stir processing. *Mater. Des.* **2012**, *39*, 358–365. [CrossRef]
42. Deepak, D.; Sidhu, R.S.; Gupta, V.K. Preparation of 5083 Al-SiC surface composite by friction stir processing and its mechanical characterization. *Int. J. Mech. Eng.* **2013**, *3*, 1–11.
43. Bauri, R.; Ram, G.J.; Yadav, D.; Kumar, C.S. Effect of process parameters and tool geometry on the fabrication of Ni particles reinforced 5083 Al composite by friction stir processing. *Mater. Today Proc.* **2015**, *2*, 3203–3211. [CrossRef]
44. Hosseini, S.A.; Ranjbar, K.; Dehmolaei, R.; Amirani, A.R. Fabrication of Al5083 surface composites reinforced by CNTs and cerium oxide nanoparticles via friction stir processing. *J. Alloys Compd.* **2015**, *622*, 725–733. [CrossRef]
45. Kumar, C.S.; Yadav, D.; Bauri, R.; Ram, G.J. Effects of ball milling and particle size on microstructure and properties 5083 Al–Ni composites fabricated by friction stir processing. *Mater. Sci. Eng. A* **2015**, *645*, 205–212.
46. Yuvaraj, N.; Aravindan, S. Fabrication of Al5083/B4C surface composite by friction stir processing and its tribological characterization. *J. Mater. Res. Technol.* **2015**, *4*, 398–410. [CrossRef]
47. Kumar, C.S.; Bauri, R.; Yadav, D. Wear properties of 5083 Al–W surface composite fabricated by friction stir processing. *Tribol. Int.* **2016**, *101*, 284–290. [CrossRef]
48. Khan, M.; Rehman, A.; Aziz, T.; Naveed, K.; Ahmad, I.; Subhani, T. Cold formability of friction stir processed aluminium composites containing carbon nanotubes and boron carbide particles. *Mater. Sci. Eng. A* **2017**, *701*, 382–388. [CrossRef]
49. Mirjavadi, S.S.; Alipour, M.; Hamouda, A.M.S.; Matin, A.; Kord, S.; Afshari, B.M.; Koppad, P.G. Effect of multi-pass friction stir processing on the microstructure, mechanical and wear properties of AA5083/ZrO_2 nanocomposites. *J. Alloy. Compd.* **2017**, *726*, 1262–1273. [CrossRef]
50. Behnagh, R.A.; Besharati Givi, M.K.; Akbari, M. Mechanical properties, corrosion resistance, and microstructural changes during friction stir processing of 5083 aluminium rolled plates. *Mater. Manuf. Process.* **2012**, *27*, 636–640. [CrossRef]
51. Khan, M.; Rehman, A.; Aziz, T.; Shahzad, M.; Naveed, K.; Subhani, T. Effect of inter-cavity spacing in friction stir processed Al 5083 composites containing carbon nanotubes and boron carbide particles. *J. Mater. Process. Technol.* **2018**, *253*, 72–85.
52. Jain, V.K.S.; Muhammed, P.M.; Muthukumaran, S.; Babu, S.P. Microstructure, the mechanical and sliding wear behavior of AA5083–B4C/SiC/TiC surface composites fabricated using friction stir processing. *Trans. Indian Inst. Met.* **2018**, *71*, 1519–1529.

53. Owa, T.; Shimizu, Y. Fabrication and Strength Behavior of MWCNT-Reinforced 5083 Aluminium Alloy Composite via Friction Stir Processing. *Mater. Trans.* **2018**, *59*, 1798–1804. [CrossRef]
54. Jain, V.K.S.; Yazar, K.U.; Muthukumaran, S. Development and characterization of Al5083-CNTs/SiC composites via friction stir processing. *J. Alloy. Compd.* **2019**, *798*, 82–92. [CrossRef]
55. Naghshehkesh, N.; Mousavi, S.E.; Karimzadeh, F.; Ashrafi, A.; Nosko, M.; Trembošová, V.; Sadeghi, B. Effect of graphene oxide and friction stir processing on microstructure and mechanical properties of Al5083 matrix composite. *Mater. Res. Express* **2019**, *6*, 106566. [CrossRef]
56. Prabhakar, G.V.N.B.; Kumar, Y.P.; Kumar, P.D.; Kumar, B.P.; Raju, M.G.; Naseema, S.; Kumar, N.R.; Jagannatham, M.; Sunil, B.R. Producing Al5083-CNT composites by friction stir processing: Influence of grain refinement and CNT on mechanical and corrosion properties. *Mater. Today Proc.* **2019**, *15*, 44–49. [CrossRef]
57. Papantoniou, I.G.; Markopoulos, A.P.; Manolakos, D.E. A new approach in surface modification and surface hardening of aluminium alloys using friction stir process: Cu-reinforced AA5083. *Materials* **2020**, *13*, 1278. [CrossRef]
58. Khodabakhshi, F.; Gerlich, A.P.; Simchi, A.; Kokabi, A.H. Hot deformation behavior of an aluminum-matrix hybrid nanocomposite fabricated by friction stir processing. *Mater. Sci. Eng. A* **2015**, *626*, 458–466. [CrossRef]
59. Khodabakhshi, F.; Simchi, A.; Kokabi, A.; Nosko, M.; Švec, P. Strain rate sensitivity, work hardening, and fracture behavior of an Al-Mg TiO_2 nanocomposite prepared by friction stir processing. *Mater. Trans. A* **2014**, *45*, 4073–4088. [CrossRef]
60. Zangabad, P.S.; Khodabakhshi, F.; Simchi, A.; Kokabi, A.H. Fatigue fracture of friction-stir processed Al–Al_3Ti–MgO hybrid nanocomposites. *Int. J. Fatigue* **2016**, *87*, 266–278. [CrossRef]
61. Khodabakhshi, F.; Nosko, M.; Gerlich, A.P. Effects of graphene nano-platelets (GNPs) on the microstructural characteristics and textural development of an Al-Mg alloy during friction-stir processing. *Surf. Coat. Technol.* **2018**, *335*, 288–305. [CrossRef]
62. Bharti, S.; Ghetiya, N.D.; Dutta, V. Investigating microhardness and wear behavior of Al5052/ZrO_2 surface composite produced by friction stir processing. *Mater. Today Proc.* **2021**, *44*, 52–57. [CrossRef]
63. Fouladi, S.; Abbasi, M. The effect of friction stir vibration welding process on characteristics of SiO_2 incorporated joint. *J. Mater. Process. Technol.* **2017**, *243*, 23–30. [CrossRef]
64. Zayed, E.M.; El-Tayeb, N.S.M.; Ahmed, M.M.Z.; Rashad, R.M. Development and characterization of AA5083 reinforced with SiC and Al_2O_3 particles by friction stir processing. In *Engineering Design Applications*; Springer: Cham, Switzerland, 2019; pp. 11–26.
65. Moustafa, E.B.; Melaibari, A.; Alsoruji, G.; Khalil, A.M.; Mosleh, A.O. Tribological and mechanical characteristics of AA5083 alloy reinforced by hybridising heavy ceramic particles Ta2C & VC with light GNP and Al2O3 nanoparticles. *Ceram. Int.* **2022**, *48*, 4710–4721.
66. Ostovan, F.; Amanollah, S.; Toozandehjani, M.; Shafiei, E. Fabrication of Al5083 surface hybrid nanocomposite reinforced by CNTs and Al_2O_3 nanoparticles using friction stir processing. *J. Compos. Mater.* **2020**, *54*, 1107–1117. [CrossRef]
67. Amra, M.; Ranjbar, K.; Dehmolaei, R. Mechanical properties and corrosion behavior of CeO_2 and SiC incorporated Al5083 alloy surface composites. *J. Mater. Eng. Perform.* **2015**, *24*, 3169–3179. [CrossRef]
68. Yuvaraj, N.; Aravindan, S. Wear characteristics of Al5083 surface hybrid nano-composites by friction stir processing. *Trans. Indian Inst. Met.* **2017**, *4*, 1111–1129. [CrossRef]
69. Soleymani, S.; Abdollah-Zadeh, A.; Alidokht, S.A. Microstructural and tribological properties of Al5083 based surface hybrid composite produced by friction stir processing. *Wear* **2012**, *278*, 41–47. [CrossRef]
70. Kurt, H.I. Influence of hybrid ratio and friction stir processing parameters on ultimate tensile strength of 5083 aluminum matrix hybrid composites. *Compos. B Eng.* **2016**, *93*, 26–34. [CrossRef]
71. Raheja, G.S.; Singh, S.; Prakash, C. Development of hybrid Gr/SiC reinforced AMCs through friction stir processing. *Mater. Today Proc.* **2020**, *50*, 539–545. [CrossRef]